Canadian Science Publishing

ARTICLE

The vulnerability of tidal flats and multi-channel estuaries to dredging and disposal

Wout M. van Dijk, Jana R. Cox, Jasper R.F.W. Leuven, Jelmer Cleveringa, Marcel Taal, Matthew R. Hiatt, Willem Sonke, Kevin Verbeek, Bettina Speckmann, and Maarten G. Kleinhans

Abstract: Shipping fairways in estuaries are continuously dredged to maintain access for large vessels to major ports. However, several estuaries worldwide show adverse side effects to dredging activities, in particular affecting morphology and ecologically valuable habitats. We used physical scale experiments, field assessments of the Western Scheldt estuary (the Netherlands), and morphodynamic model runs to analyse the effects of dredging and future stresses (climate and sediment management) on a multi-channel system and its ecologically valuable intertidal flats. All methods indicate that dredging and disposal strategies are unfavourable to long-term morphology because dredging creates and propagates the imbalance between shallow and deeper parts of the estuary, causing a loss of valuable connecting channels and fixation of the tidal flats and main channel positions, while countering adverse effects by disposal strategy has limited effectiveness. Changing the disposal strategy towards main channel scour disposal can be economically and ecologically beneficial for the preservation of the multi-channel system. Further channel deepening will accelerate the adverse side effects, whereas future sea-level rise may revive the multi-channel system.

Key words: estuary, dredging and disposal, tidal flats, multi-channel system, flume experiments, morphodynamics.

1. Introduction

River mouths, or estuaries, are important centres of global transportation and commerce. Most estuaries have been continuously dredged since the early 20th century with an acceleration of activity in the last decades. Continuous dredging is necessary to

Received 5 June 2020. Accepted 30 November 2020.

W.M. van Dijk. Department of Physical Geography, Faculty of Geosciences, Utrecht University, Utrecht, the Netherlands; Water & Environment Division, Arcadis, Zwolle, the Netherlands.
J.R. Cox and M.G. Kleinhans. Department of Physical Geography, Faculty of Geosciences, Utrecht University, Utrecht, the Netherlands.
J.R.F.W. Leuven. Department of Physical Geography, Faculty of Geosciences, Utrecht University, Utrecht, the Netherlands; Department of Rivers and Coasts, Royal HaskoningDHV, Nijmegen, the Netherlands; Department of Environmental Sciences, Wageningen University, Wageningen, the Netherlands.
J. Cleveringa. Water & Environment Division, Arcadis, Zwolle, the Netherlands.
M. Taal. Department of Marine and Coastal Systems, Deltares, Delft, the Netherlands.
M.R. Hiatt. Department of Physical Geography, Faculty of Geosciences, Utrecht University, Utrecht, the Netherlands; Department of Oceanography and Coastal Sciences, College of the Coast and Environment, Louisiana State University, Baton Rouge, LA, USA; Coastal Studies Institute, Louisiana State University, Baton Rouge, LA, USA.
W. Sonke, K. Verbeek, and B. Speckmann. Department of Mathematics and Computer Science, TU Eindhoven, Eindhoven, the Netherlands.
Corresponding author: Wout M. van Dijk (email: wout.vandijk@arcadis.com).

maintain navigation depth, so commercial vessels, which are increasing in size and number, can access major ports now and in the future (De Vriend et al. 2011) in, e.g., the Yangtze Estuary (Shanghai, Chen et al. 2016), the Western Scheldt (Antwerp, Jeuken and Wang 2010; Wang et al. 2015), and the Elbe Estuary (Hamburg, Kerner 2007). The demand shipping places on estuaries also poses considerable issues for the sustainability of these estuaries (Best 2019). Dredging smoothes the estuary and obstructions to ships, e.g., shoals, bars, and sills are removed (Nichols 2018), which affect smaller channels and bars that are important for seabed animals, fish, and birds. The hydrodynamic effects of dredging include tidal amplification (Temmerman et al. 2013; Zhu et al. 2015), which increases circulation and increases the flood dominance of the tidal asymmetry (Van Maren et al. 2015). It is site-specific which hydrodynamic processes dominate and how these combine with the effects of dredging and dumping to affect sediment transport and the morphodynamics of the system. Moreover, dredging activities are thought to cause a shift from a multi-channel system to a single-channel system (Wang et al. 2011; Monge-Ganuzas et al. 2013) and a loss of ecologically valuable intertidal flats (Essink 1999; Liria et al. 2009; De Vriend et al. 2011; Temmerman et al. 2013; Yuan and Zhu 2015; Van der Wal et al. 2017). Yet, it remains undiscovered what the long-term effects of the current dredging and disposal strategies have on the sustainability of tidal flats and multi-channel estuaries, and what the response will be from future stresses such as increasing minimum channel depth for shipping and sea-level rise (SLR).

The ecological quality of multi-channel systems is partly determined by the presence and characteristics of intertidal flats and channels (Toffolon and Crosato 2007). Multi-channel systems often display a quasi-regular repetitive pattern that consists of meandering ebb-dominated channels and straight flood-dominated channels in the inner bends (Jeuken 2000; Winterwerp et al. 2001). The difference in meander action between ebb and flood channels, and the opposite direction of residual sand fluxes in these channels lead to the formation of intertidal flats, which are dissected by connecting channels (Jeuken 2000; Toffolon and Crosato 2007; Hibma et al. 2008; Leuven et al. 2018*a*). Estuarine multi-channel systems typically consist of an ebb-dominated channel and one or more flood-dominated channels, displaying characteristic morphological behaviour that is associated with the net sediment exchange between channel junctions. Apart from their crucial ecological value, there are several important reasons to sustain the multi-channel system (of equally important ebb and flood channels) and counteract adverse effects due to dredging, namely: (*i*) side channel shallowing by disposal reduces the navigability of smaller inland vessels (Wang et al. 2015); (*ii*) main channel deepening increases tidal range and flood risk (Liria et al. 2009); (*iii*) increased peak velocity in deepened main channel affects navigability (Colby et al. 2010; Nichols 2018); (*iv*) channel deepening threatens bank stability, tidal flat stability, and salt-marsh stability (Liria et al. 2009; Van Dijk et al. 2018, 2019); and (*v*) large morphological changes alter ebb-flood dominance, including duration and asymmetry (Colby et al. 2010), potentially affecting mud and sand budgets.

Urgent research questions related to dredging and disposal in large estuaries in general are as follow: (*i*) To what degree can the multi-channel system be sustained or restored by current dredging and disposal practices? (*ii*) What are the effects of further main channel deepening on the morphology of the multi-channel system? (*iii*) What will be the effect of predicted SLR (Church et al. 2013) on the morphological and ecological functioning of the estuary? Here, we show how dredging changes the natural development of estuaries by a combination of scale experiments in the laboratory, where the effect of dredging was isolated, and data assessment from the Western Scheldt (the Netherlands) for real scale practice. We applied a numerical model to quantify how disposal strategy can limit adverse side effects, and how future scenarios, such as increasing shipping draft and SLR, will affect estuary morphodynamics and habitat suitability.

2. Methods

We use three independent, complementary methods. (*i*) In physical scale experiments, the long-term development and resilience of an estuary with dredging and disposal was compared with a reference experiment without interventions. (*ii*) Field data from the well-monitored Western Scheldt were acquired to determine the morphological development in an actual dredged estuary. Literature and available reports were used to connect morphological changes to changes in dredging and disposal strategy. (*iii*) Numerical model scenarios allowed testing of the effects of disposal strategy and future changes in dredging regime and SLR scenarios, for the case of the Western Scheldt. For all three approaches, we employ a novel channel-network algorithm that scale-independently and objectively extracts channel-network topology. Each network is then used to determine the channel depth distribution, channel migration, and the tidal flat volumes.

2.1. Physical scale experiments

Experiments with and without dredging and disposal were conducted in a periodically tilting flume: the Metronome. The flume was 20 m long and 3 m wide and had a sandy bed of 7 cm thick. Periodic tilting of the flume enabled sediment transport during both ebb and flood phase (Kleinhans et al. 2017*b*), leading to autogenic development of estuarine morphodynamics (Braat et al. 2018; Leuven et al. 2018*a*). A single tidal cycle spanned 40 s and had a maximum tilting gradient of 0.008 m/m. Further information on scaling is reported in earlier papers (Kleinhans et al. 2017*b*; Braat et al. 2018; Leuven et al. 2018*a*). Changes of the experiment were recorded by time-lapse overhead imagery, and DEMs were constructed with the structure-from-motion software, AGISOFT Photoscan (version 1.2.6.2038). The DEMs were used to calculate dredging and disposal volumes and locations. The development of the experiment with dredging was compared to a control run without dredging.

The experiment started with a narrow converging channel of uniform depth in the middle of the sand bed. The lateral boundaries were erodible, and continuous erosion and deposition by the tidal currents led to the development of a self-formed estuary before dredging and disposal were started at 3000 tidal cycles. The self-formed estuary consisted of a multi-channel system with ebb and flood channels and tidal flats. The estuary had an irregular shape with the same morphological characteristics as the control run (Leuven et al. 2018*a*). After 3000 cycles, an initial "shipping fairway" was cut along the deepest natural course of the estuary, which linked both ebb and flood channels when necessary. The shipping fairway was lowered by capital dredging by about 1/5 of the original depth using a palette knife and removal of sediment from the system by hand. The minimum depth requirement for the dredging was set to 3.5 cm for the first capital dredge, whereas for the second capital dredge, which was necessary because of the continuous rapid expansion of the estuary, the minimum depth requirement was set to 3 cm. Maintenance dredging then took place every 50–100 cycles to remove material locally which made the channel "unnavigable", in other words, when the water depth was below the minimum depth requirement. The width of the dredged main channel was proportional to the width of the estuary in the same ratios as for the field example, the Western Scheldt. For the landward end, this was approximately 10% of the estuary width, 15% moving into the middle reaches of the estuary, and at the seaward end up to about 20% of estuary width.

Sediment from the first capital dredge was removed from the system entirely to ensure the stability and persistence of the new dredged channel and new morphology which was significantly different to the control experiment. This is common practice for many channel deepening events where the material is either removed completely and sold (such as the Rhine Meuse estuary) or is placed far out of the navigation channel so it does not circulate back into the dredged regions (Elbe estuary). This was done to create a system that mimics the history and morphological development of the Western Scheldt. Sediment removed later during maintenance dredging was redistributed on the seaward side of adjacent tidal flats, at the entrance of side channels, and in the scours of the main channel that had a depth >4 cm. Material placed on tidal flats bars and shoals was placed at the edges where elevation was lowest/the shallowest part of these features so it was easily subject to remobilisation. The disposal location depended solely on proximity to the dredging site. After the final maintenance dredging event (at 5200 tidal cycles), the estuary was allowed to evolve further without interference for 8000 cycles until termination of the experiment at 13 000 tidal cycles.

2.2. Field case study

For reasons of data availability, this study uses the Western Scheldt as example, which is located in the southwestern part of the Netherlands. The study area is the seaward section (60 km) of the tide-dominated Scheldt estuary that is 200 km long and stretches up to Gent in Belgium (Fig. 1*a*). The Western Scheldt is characterised as a multi-channel system, with well-developed channels and shoals. It has on average a convergent geometry and covers an area of about 370 km^2. The main driving force of the system is the tide. From the mouth of the estuary to the middle reaches at the Dutch/Belgian border, the tidal range increases from 3.5 to 5 m (Jeuken 2000). The tidal prism at the mouth is about 1 billion m^3, whereas the yearly-averaged river discharge of the Scheldt into the Western Scheldt is a morphologically negligible 120 m^3/s, causing the estuary to be well mixed (Cancino and Neves 1999; De Vriend et al. 2011). Relatively fine sediment is found in the Western Scheldt: the median grain size D_{50} of the channel bed varies between about 150 and 300 μm. Mud is limited to thin layers on mud flats (Van de Lageweg et al. 2018). The Western Scheldt provides access to various harbours, of which the port of Antwerp (Belgium) is the largest, and both the main and side channels are used by various ships.

The Western Scheldt is an estuary that has undergone human interference since dikes were introduced in the 14th century, which has reduced its lateral expansion capacity. At the beginning of the 20th century, small-scale sand mining, dredging, and disposal became the foci of human activity which has intensified since the 1970s (Van der Spek 1997). The Western Scheldt has undergone three major deepening events (in the 1970s, 1990s, and 2010s) as well as annual maintenance dredging activities to allow access to the port of Antwerp. The current maintained navigation depth is 14.5 m below Lowest Astronomical Tide (LAT). Disposal locations are chosen such that costs, efforts, and hindering navigation are minimised and thus selected in the vicinity of dredging locations (MOW 2013). The dredging and disposal strategy was changed in 2010 from straightforward disposal in the side channels and deeper parts of the main channel to an alternative "flexible" approach in which sediment is disposed near eroded intertidal flats. This new "flexible disposal" approach for the Western Scheldt includes monitoring and adjustment when necessary. Disposal at intertidal flats allows slow movement of material towards the flats with the aim of enhancing subtidal and intertidal habitats (De Vriend et al. 2011) and decreases disposal intensity in the side channels that began to close off (Roose et al. 2008). The intention was to maintain and preserve the equilibrium of the multi-channel system of the Western Scheldt, attain maximum ecological gain on the edges of inter-tidal flats and preserve the ecologically valuable habitats of the Western Scheldt (Depreiter et al. 2011, 2015; De Vriend et al. 2011; Plancke et al. 2014; Vikolainen et al. 2014).

Fig. 1. (*a*) The 2014 bed elevation (courtesy of Rijkswaterstaat) of the Western Scheldt plotted on top of a Landsat-8 image (courtesy of the U.S. Geological Survey). The map was created with ArcGIS. (*b*) Dredging and disposal locations for the model runs plotted as polygons on top of the bed elevation map of 2015. The disposal strategy varies between model runs, (*i*) uses all three types of disposal locations (shown by the green, light green, and white polygons, and referred to as the alternative shoal disposal), (*ii*) only two types (shown by the light green and white polygons, and referred to as the straightforward side and main channel disposal), or (*iii*) only one type (shown by the white polygon and referred to as the foreseen scour disposal). The white dashed line represents the shipping fairway and red polygons are dredging locations. The map was created in MATLAB.

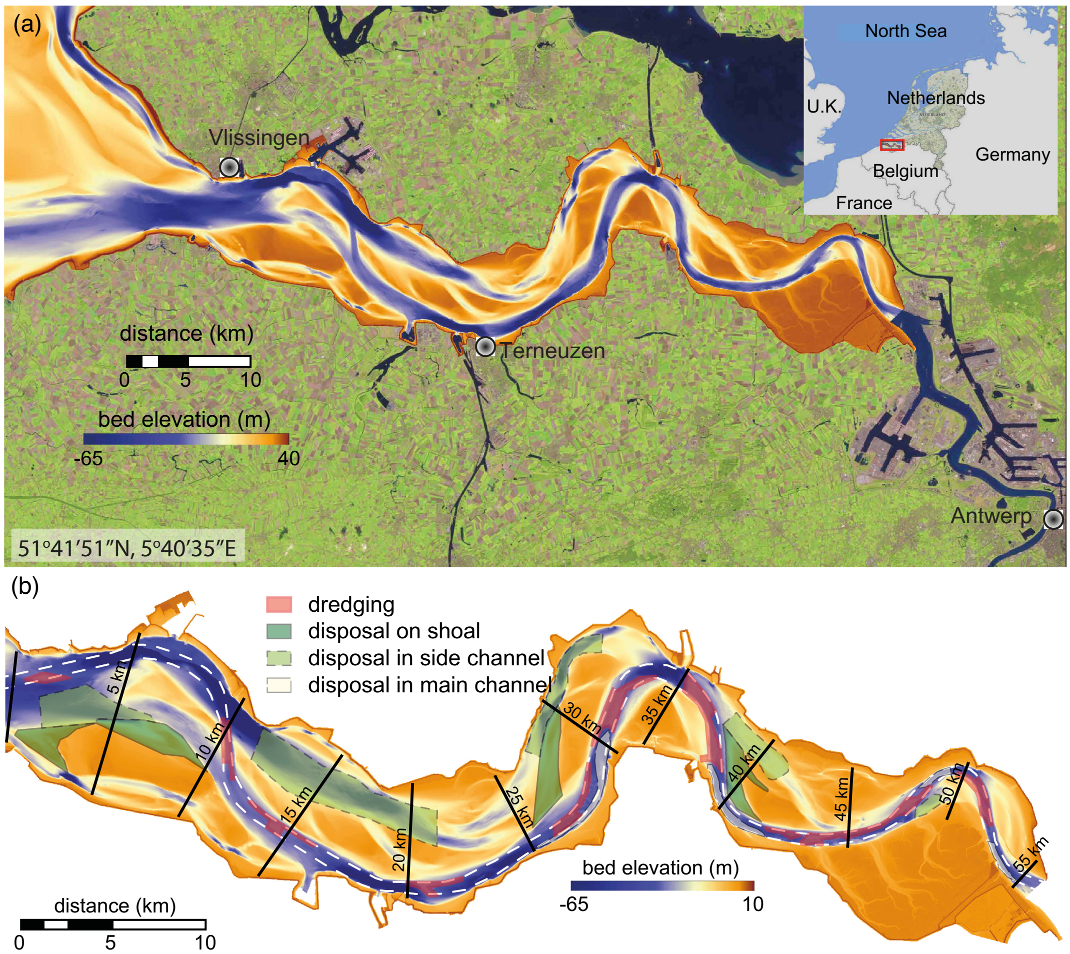

To analyse the effect of dredging and disposal strategies on the development of the Western Scheldt, bathymetry data, so called Vaklodingen, were used. These were available for the period between 1955 and 2015. The bathymetry data is created using single-beam measurements at 100–200 m transects. Positioning and height measurements were done with a number of analogue to digital techniques (Cleveringa 2013). Since 2001, the areas about the mean water elevation have been measured with lidar and have a higher resolution of 1–5 m. The vertical accuracy of the dataset for practical use was set at 10 cm (2σ, see Elias et al. 2017). The bathymetry data of the Western Scheldt were utilised here for network extraction, which we used to calculate channel dynamics, depth, and tidal flat volumes. Additionally, we determined the intertidal flat elevation and area by comparing bed elevation distributions of the tidal flats over time. While field experiments and monitoring provide valuable insights, the lack of a control scenario inhibits the clear conclusions which are possible using controlled experimentation such as physical scale experiments and with numerical scenario modelling introduced below.

2.3. Numerical morphodynamic modelling

Here, we used the numerical model Delft3D to simulate fluid flow and morphological changes over time. Delft3D has widely been applied to simulate rivers, estuaries, and tidal basins (Lesser et al. 2004; Schuurman et al. 2013; Van Dijk et al. 2019). Our runs were computed using depth-averaged, nonlinear, shallow-water equations, wherein the effect of helical flow driven by flow curvature on bed shear-stress direction was parametrised (Schuurman et al. 2013). The associated transverse bed slope effect is defined as sediment on a slope transverse to the main flow direction. This sediment is deflected downslope due to gravity, and, when a secondary current is present as in bends, the inward and upslope directed shear stress drags particles upslope. The transverse bed slope is a tuning parameter that sets the morphological shape of the channel. We applied the method of Bagnold for the transverse sediment transport component, and we set the tuning parameter for the transverse bedload transport, α_{bn} to 30, so that realistic bed slopes for long-term simulations were maintained (Baar et al. 2019).

The Delft3D schematisation was based on the optimised NeVla-Delft3D model for hydrodynamics (Hartsuiker 2004; Vanlede et al. 2009; Vroom et al. 2015) and morphology (Schrijvershof and Vroom 2016) of the Scheldt estuary. This NeVla-Delft3D model is the most accurate model available for the study area, it has however, limitations as it is not cannot accurately represent morphological changes over decadal timescales and the distribution of dredging activities are not verified. Therefore, we compared our findings against a control run, and focus on scenario analysis including changes in the channel network. We used a nested flow model from the NeVla-Delft3D model (NeVla: Nederlands–Vlaams/Netherlands–Flemish) for reducing computational time (Van Dijk et al. 2019). The sediment transport formula included is Van Rijn (2007*a*, 2007*b*), and the roughness field in the model is defined by Manning *n* and is variable over the model domain (Maximova et al. 2009*a*, 2009*b*, 2009*c*; Vroom et al. 2015). The Manning *n* varies between 0.022 ($s/m^{1/3}$) for the eastern part, 0.027 ($s/m^{1/3}$) for the western part, and 0.028 ($s/m^{1/3}$) for the Verdronken Land van Saeftinghe.

The nested model consists of a curvilinear grid with varying grid size, and we validated the nested model to the original calibrated NeVla-Delft3D model (see Supplementary Material[1]). The boundaries of the nested model include a water level fluctuation due to tides at the seaward boundary and a discharge at the landward boundary. Sediment was uniform with a median grain size of 200 μm, comparable to field observations (Van Dijk et al. 2019). For simplification of the boundary conditions, these were selected from a single spring-neap tide cycle of January 2013 (about 14 days), which was repeated for a two-year period. We speed up the bed adjustments by multiplying the morphological change during hydrodynamics timesteps by a factor (*M*) of 20. In some places, the thickness of the bed is limited by underlying non-erodible layers from Holocene and Tertiary deposits (Gruijters et al. 2004; Dam 2017; Van de Lageweg et al. 2018). Sediment transport at the boundaries is in an equilibrium state with the flow and is unlimited. Several processes are excluded, including wind (direction and magnitude) and salinity, to reduce computational time. Here, we assumed that in the long-term, these processes are negligible for the large-scale and

[1]Supplementary material is available with the article at https://doi.org/10.1139/anc-2020-0006.

long-term morphological development, although water levels with and without salinity can differ by about 0.1 m (Smolders et al. 2016).

Numerically, it is not practically possible to apply a flexible approach in which yearly the disposal locations are shifted. Instead, we isolated the effects of three fixed strategies on the long-term development that represent the approaches in reality. These include (*i*) a straightforward approach were dredged sediment is disposed equally between the main and side channel; (*ii*) an alternative scenario, as applied from 2010 and onwards, in which dredged sediment is distributed for 20% on the tidal flats, 38% in the side channels, and 42% in the scours of the main channel; and (*iii*) a foreseen approach were solely sediment is disposed in the scours of the main channel, as proposed for future strategies. To limit the amount of variation between the three scenarios, we did not adjust the disposal polygons for the third scenario. Furthermore, for simplification, the dredged sediment was not distributed in the nearest disposal polygon as done in reality nor adjusted over time to reduce possible unrealistic long-term morphological impacts. Here, the dredged sediment is distributed over all polygons according to the percentage given above. The maintained dredge depth was set to 14 m, i.e., dredging takes place when water depth is less than 14 m, and dredging was concentrated at nine sill locations (see polygons in Fig. 1*b*).

For further testing of future scenarios, we performed some additional runs for the first scenario with increasing maintenance depth of 16, 18, and 20 m. Additionally, we ran the model with three scenarios of SLR (1, 2, and 3 mm/year) to test the effectiveness of dredging against future SLR scenarios (as in Church et al. 2013; Van de Lageweg and Slangen 2017). By using a wide range of values, we implicitly study the sensitivity of the SLR predictions (Van de Lageweg and Slangen 2017). The SLR was simulated by increasing the downstream water level boundary with a rate of the simulated SLR.

2.4. Data analysis

For the data analysis of the multi-channel network, we applied a novel, mathematically rigorous framework for extraction of multi-threaded channel networks from topographic surfaces (developed by W. Sonke called Topological Tools for Geomorphological Analysis, TTGA; Kleinhans et al. 2017*a*, 2019; Hiatt et al. 2020). In contrast to previous methods with manual operations or subjective choices, this framework automatically captures network topology with channel bifurcations, confluences, and channels of various sizes. The method is scale-independent and uses only bed elevation as input, so it works independently from water surface elevation. For the analysis in this paper, we used a slightly modified version of the original framework, which emphasises locally recognised channels over than the original algorithm. This local approach results more stable attribution of channel size, which is hence better suited for the analysis of channel networks, with a range of channel sizes that evolve over time.

The underlying algorithm computes the Morse-Smale complex (MSC) of the terrain (Edelsbrunner et al. 2001; Kleinhans et al. 2019; Hiatt et al. 2020), a topological complex that describes the structural elements of the terrain. The MSC contains the local minima, maxima, and saddle points (points that are a local minimum in one direction and a local maximum in the other), along with steepest-descent paths (called MS-edges) from each saddle point towards a minimum. These MS-edges partition the terrain into pieces (called MS-cells), each representing a local maximum with the descending area around it. The algorithm proceeds by gradually merging insignificant MS-cells together to form larger, significant cells, each representing a tidal flat/shoal in the channel network. The remaining MS-edges around those cells then form the channels. Whether a cell is significant or not is determined by the volume of sediment contained in the cell: we keep merging cells until the volume in each cell is larger than some fixed threshold δ. This implies that channels are separated by at least volume δ, which is morphologically meaningful, because this volume is related to the morphological work required to cut shoals and merge channels (e.g., Kleinhans 2005). By running the method for different threshold values δ, we obtain networks with more and fewer paths, from which main, side, and connecting channels can be extracted. The main channel is the path with a maximum value for δ as there are no tidal flats enclosed. Side channels are the channels that are connected to the main channel or other side channels at both ends, and connecting channels are the channels that connect the side with the main channel. If we start with a low threshold δ, and then gradually increasing δ, channels disappear from the network one by one. We annotate each channel in the network by the highest threshold value δ for which that channel still appears in the network. That is, the threshold value for a channel represents the volume of the smaller of the two adjacent tidal flats.

The extracted channel network provides, in addition to the location of channels of various scales, the opportunity to determine the channel dynamics and the channel depth per channel scale. To compute statistics on the tidal flat volumes, we used the channel network for a fixed threshold value δ of 100 000 m^3. The tidal flat volume was calculated by the summation of the bed elevation above the cross-sectional median bed elevation along the estuary. The median bed elevation was determined by the same method as Leuven et al. (2018*b*). First, a centreline was defined as the mean location line between the boundaries of the estuary. Second, the centreline was smoothed and resampled at an interval of 200 m. At each resampled point, a cross-section was constructed with a 20 m transverse grid spacing, perpendicular to the centreline and within the boundaries of the estuary. Then, the median bed elevation was determined for each cross-section, and a linear regression was fitted to the median bed elevation along the estuary channel. Elevation above the regression line was included for the tidal flat volume within the channel network. Afterwards, the 20th, 50th, and 80th percentiles were calculated as representations of channels, intermediate, and high bed elevations. Below we provide a few examples of how dynamics are determined, show depth distributions of identified channels and show the cumulative distribution of tidal flat volumes (using the volume parameter, δ (Kleinhans et al. 2019; Hiatt et al. 2020)).

3. Results

3.1. Experimental development of a multi-channel estuary

The experiment in the Metronome with dredging and disposal was conducted in similar conditions as an undredged control experiment that showed three phases of development. First, alternate bars, i.e., shoals, developed during widening of the estuary. The initial alternate bars grew and flanked a meandering channel, comparable to alternate bars in rivers. As soon as the bars exceeded a width-to-length ratio of approximately 1/7, the flood flow carved a barb channel, which is a one-ended channel that partly crosscuts a bar. This is analogous to a chute channel in a meandering river. The seaward barb channels progressively cut through the alternate bars, while the bended channels expanded laterally. The resulting estuary shape had a structure (as described by Van Veen 1948) with mutually evasive ebb- and flood-dominated channels, similar to the Western Scheldt.

In the second phase, mid-channel bars formed that were large enough to divert the flow, accelerate outer-bend erosion, and form major bifurcations and confluences seaward and landward of the mid-channel bars. A quasi-periodic estuary planform formed, where, at the confluence locations, the estuary width remained generally narrow and dynamic channels and bars only occurred within a small stretch of the estuary width. During this phase, dredging was started in the new experiment presented here (Fig. 2, top panel). This

Fig. 2. Estuary evolution of the experiment illustrated by bed elevation maps without (left panels) and with dredging (right panels) overlain by the extracted channel network. The sub-, inter-, and supratidal area are based on water level measurements. Note that tidal flats with elevation above high-tide level are referred to as supratidal and those with an elevation below low-tide level are classified as subtidal (Desjardins et al. 2012). The map was created in MATLAB.

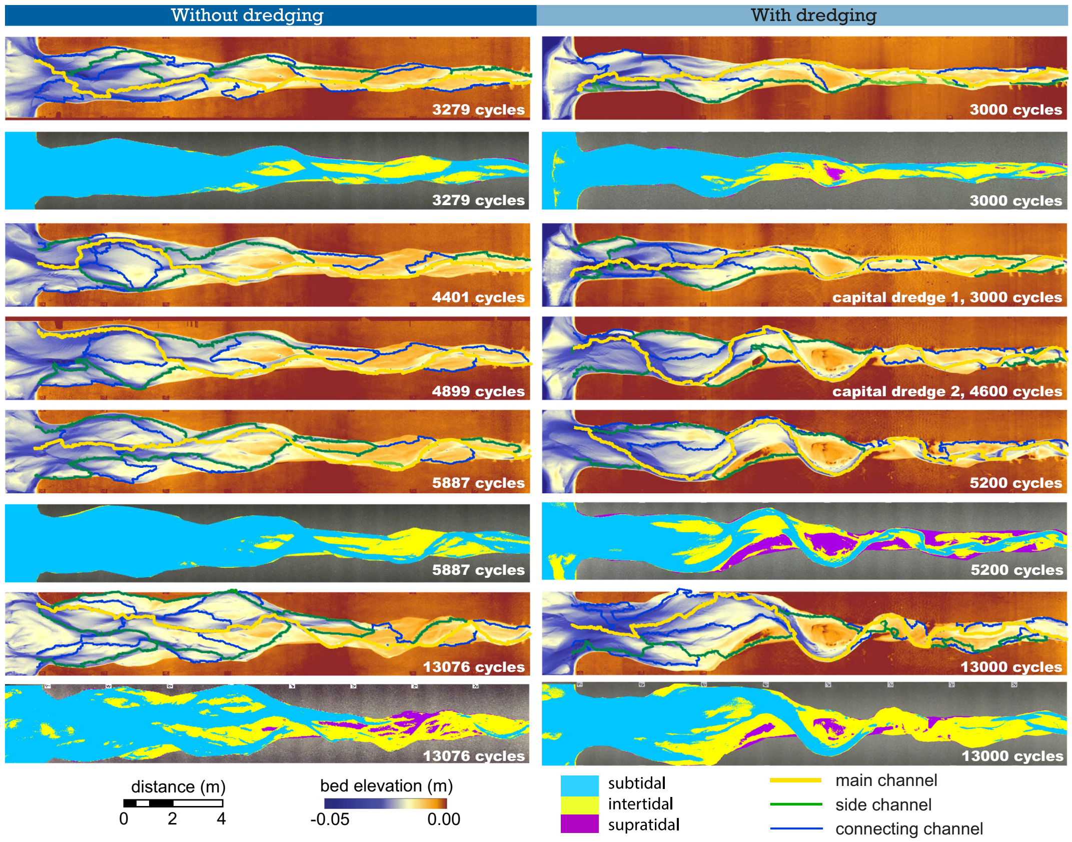

required the cutting of an initial shipping fairway after 3000 cycles, i.e., a single main channel, which connected ebb and flood channels to follow the naturally deepest course.

In the third phase, further extension of the outer bends made the mid-channel bar favourable for a shortcut during both the ebb and flood flows. New barb channels formed on the mid-channel bars, which cross-cut the bar forming a new main channel in the middle of the estuary (Fig. 2, left panel, 4401–5887 tidal cycles). Due to dredging and accompanying disposal of dredged sediment on the shoal in the middle of the flume, the meander bend became fixed, only migrating in a lateral direction. Because of this high shoal, the water level no longer exceeds shoal elevation and no new barb channels formed (Fig. 2, right panel, 4600–5200 tidal cycles). In the first capital dredge, the largest amount of sediment was dredged, with the highest volumes in the seaward half. During maintenance and the second capital dredge, the dredging activity was concentrated in the middle of the flume (Fig. 3*a*).

After the final maintenance dredging event (5200 tidal cycles), the estuary was allowed to evolve for a further 8000 cycles until it was terminated at 13 000 tidal cycles. The lateral migration of the bend in the middle of the flume continued even when dredging stopped,

Fig. 3. (*a*) Dredging volumes along the experiment vary spatiotemporally and are especially large during the two capital dredging events. Higher dredging volumes were observed more landwards and peaked between 8 and 12 m. (*b*) Location of the main channel in the experiment with and without dredging. The map was created in MATLAB.

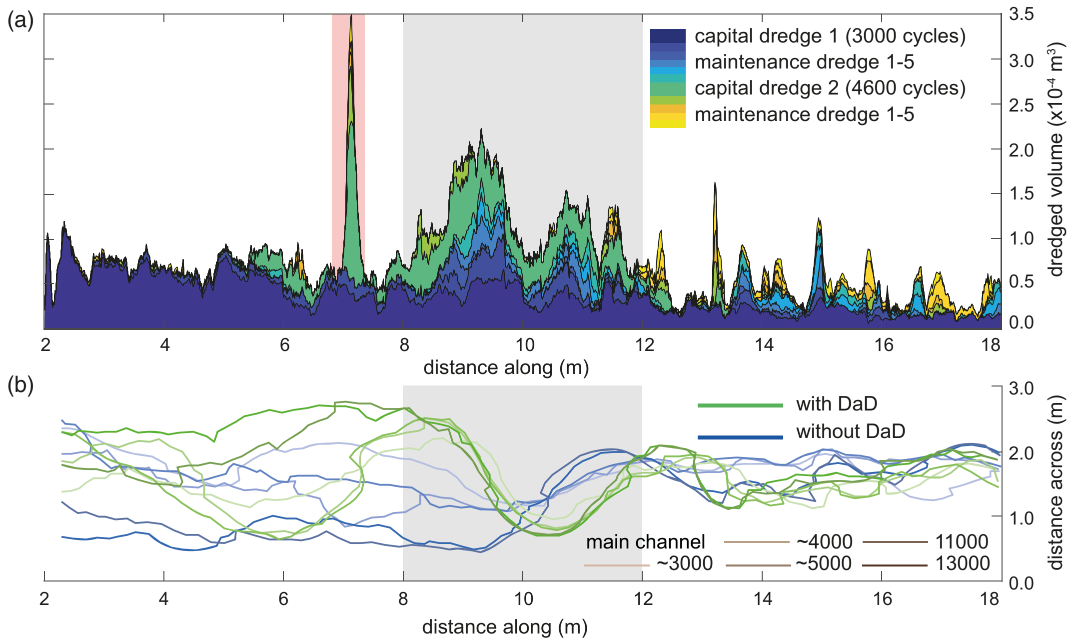

whilst seaward mid-channel bars were cross-cut. Eventually, a dynamic equilibrium at the bar-confluence scale was reached, in which sediment from bars and banks was reworked into new bars within the estuary. In both experiments, with and without dredging, the quasi-periodic planform deviated from the ideal estuary shape, which describes estuaries as exponentially converging channels, at the end of the experiments (Fig. 2, bottom). In general, the experiments confirm that the shoal elevation and size increased and channel dynamics decreased due to dredging and disposal. Figure 3*b* indicates that the location of the big meander remained stable in the dredged experiment, even though dredging ended after 5200 tidal cycles. The Supplementary Videos 1 and 2[1] present the development of the two experiments observed from the overhead cameras.

3.2. Western Scheldt

Various sediment budgets for the Western Scheldt have been published, based on the available Vaklodingen datasets, information on the dredging and disposal, and sand mining volumes and assumptions on the boundary conditions of transport to the Sea Scheldt and Land van Saeftinghe tidal marsh complex. Considering the accuracy of the data, trends in the developments of the sediment volume are of greater interest in this context than the year-to-year variations. The resulting sediment budget shows three periods with comparable trends (Cleveringa 2013). These periods do not coincide with the intervals between major deepening events, but instead represent slower trends in sediment volumes and the changing strategies for dredging, disposal, and sand mining. In general, in the first period (1955–1976), dredging was limited to the eastern half, while sediment volume decreased in the entire Western Scheldt. In the second period (1976–1994), dredging volume

Fig. 4. (*a*) Dredging and disposal volumes per year in the Western Scheldt which show an increase from 1970 onward. (*b*) Channel location determined by the network extraction method for the Western Scheldt since 1960. Colours show the different channel scales, and brightness indicates the year in the observation period. The map was created in MATLAB.

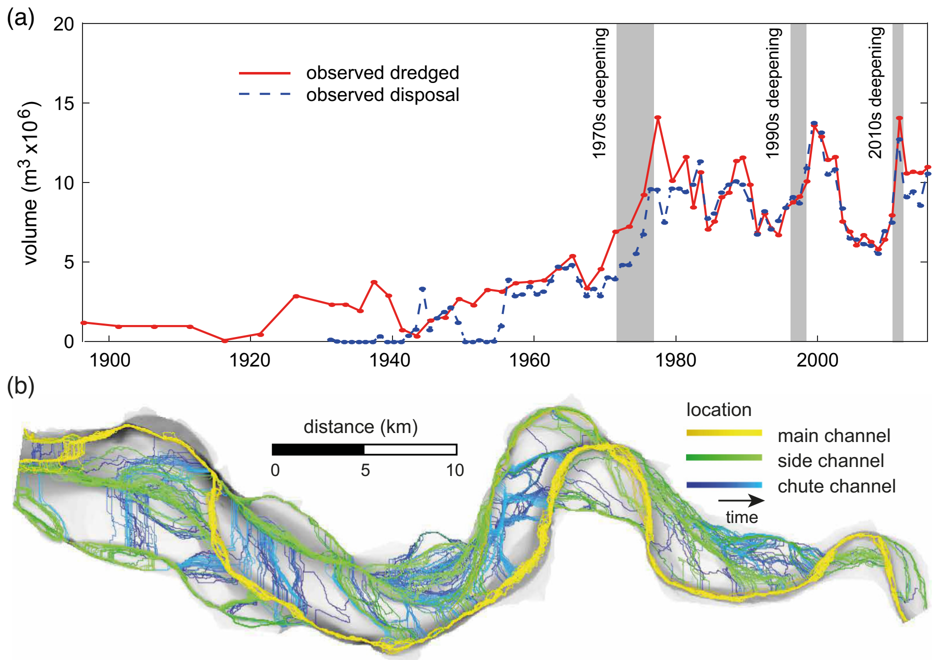

increased in the entire Western Scheldt. Most material was dredged in the eastern half, while sediment was no longer displaced from the western half to the eastern half or visa versa. In the third period (1994–2010), dredged sediment was transported from east to west, which altered the sediment budget of our study area.

Analysis of the yearly bathymetry of the Western Scheldt demonstrates that the main channel shows limited variation since 1955 (Fig. 4*b*). Only around 1960, the course of the main channel shifted at one location to the side channel and has not shifted back since, creating a new main course. This shift was not related to dredging activities. There is more variation over time in the side and connecting channels (Fig. 4*b*). From the observations, it is clear that a few locations were not covered by any channel over the 60 year period. These stable tidal flats became larger over time due to amalgamation of tidal flats (Figs. 5*a* and 5*b*). The field observations show that, at stable tidal flat locations, the surface area has increased since 1955 for almost all tidal flats (Fig. 5*c*). Also, the elevation of these tidal flats has increased since 1955 (Fig. 5*d*). The increase in tidal flat height is partly the result of high water level increase (Temmerman et al. 2004).

3.2.1. Numerical model

Model simulations were employed to determine effects of different disposal scenarios as well as future stresses. Three disposal scenarios were tested. The channel dynamics for the different disposal strategies show a clear difference between the control run (without dredging) and the different dredged scenarios (Fig. 6). Because of dredging, the main channel becomes more fixed than in the control run without dredging. The side and connecting channels show some shifts between the disposal strategies, but there is no

Fig. 5. Shoal development in the Western Scheldt from 1955 to 2017. (*a* and *b*) Ongoing merging of tidal flats, from fragmented shoal complexes (*a*) to 2–3 large tidal flats per meso-cell (*b*). (*c*) Difference in the shoal surface area with respect to 1955 shows an increase in tidal flat area for all locations. (*d*) Average tidal flat height difference with respect to 1955 shows an increase at all tidal flat locations. The map was created in ArcGIS.

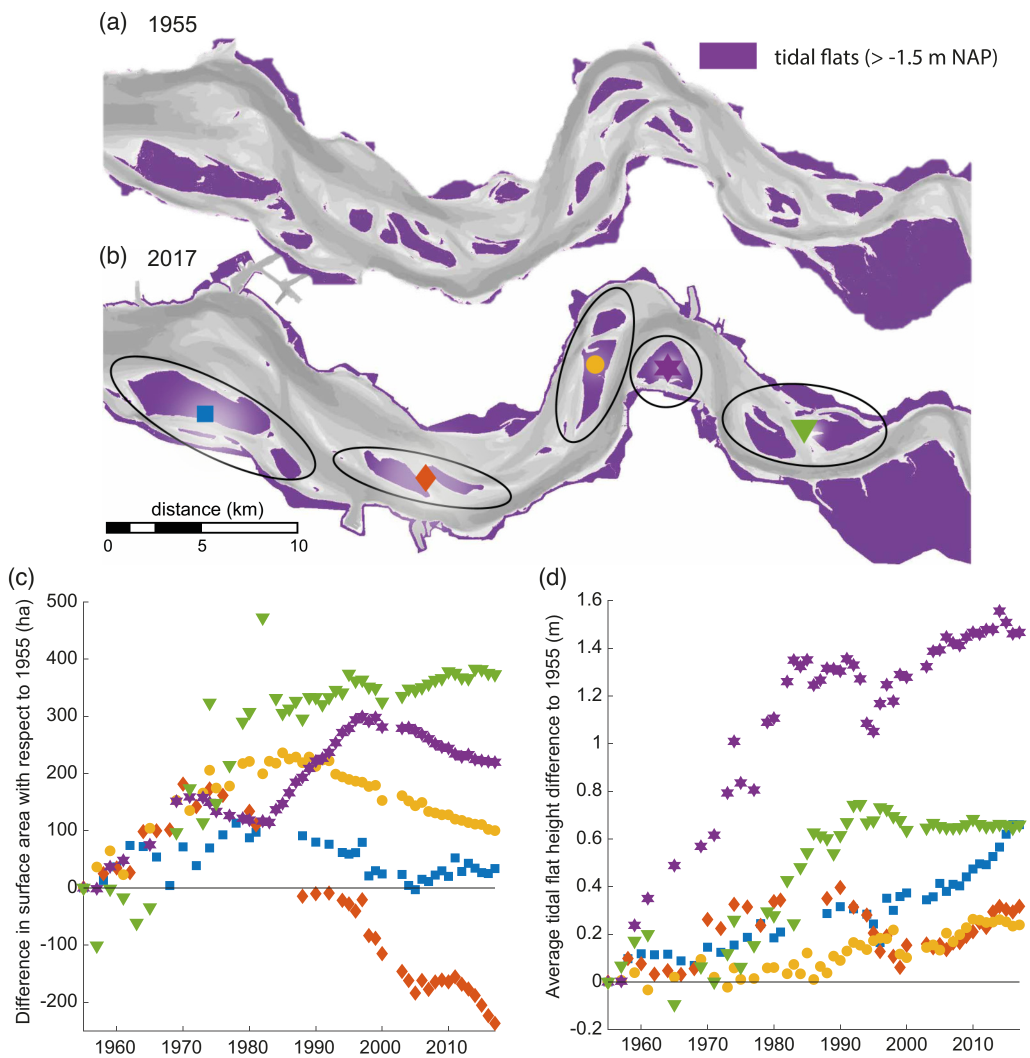

clear distinctive effect of the different disposal strategies (Figs. 6*b*–6*d*). The tidal flats distinguished between the channels are comparable in size and number between the simulations.

See Supplementary Videos 3–5[1] for the channel locations over time for the model simulations.

Future scenarios with increased navigation depths and SLR were also assessed. Where navigation depth for shipping increases and thus dredging depth increases, the model shows that the channel location for the various scales is more fixed (Fig. 7). In particular, the total surface area that is covered by the main and side channel decreases with increasing depth of dredging. Conversely, the SLR scenarios show that the surface area covered by channels increases with increasing SLR rate: higher water levels are more likely to carve

Fig. 6. Channel locations for different dredging strategies determined by the network extraction method for the model runs. (*a*) Control run without dredging and disposal (DaD, dredging and disposal). Channel network over time for the different disposal strategies, including (*b*) straightforward approach, (*c*) alternative approach, and (*d*) the foreseen approach. The map was created in MATLAB.

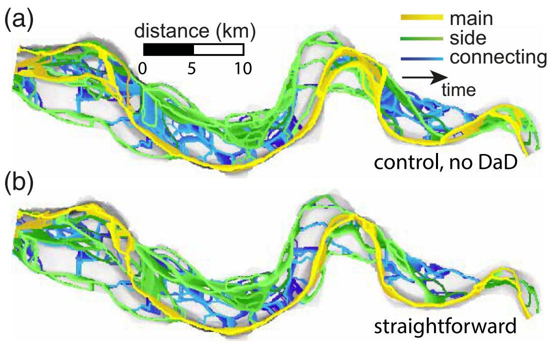

Fig. 7. Channel locations determined by the network extraction method for the model runs with different dredging depths. (*a*) Control run with dredging depth of 14 m. (*b*) Dredging depth of 16 m. (*c*) Dredging depth of 18 m. (*d*) Dredging depth of 20 m. The map was created in MATLAB.

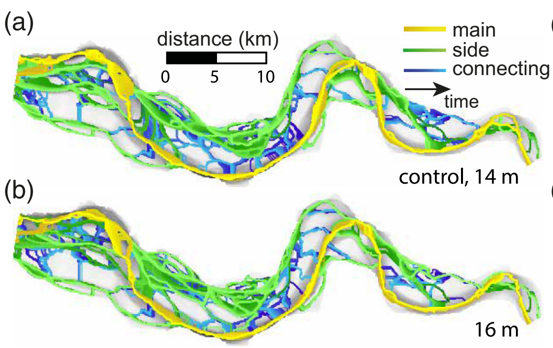

and erode channels. This is particularly the case for the side channels and the connecting channels, but less so for the main channel that seems more fixed to its current location (Fig. 8).

The dredging volumes are equal for all the disposal strategies in the first years, but the three strategies begin to deviate after 10 morphological years (Fig. 9*a*). The dredging volume at the beginning is the result of the initial bathymetry, whilst in the later stages, as the disposal strategy determines the new bathymetry, it also controls the dredging volume. Contrary to our expectations, the required dredging volume for the disposal strategy with disposal only in the scours of the main channel is lowest for the first 25 years, as the scours get filled. The total dredged volume increases towards the end of the simulation. The alternative disposal strategy shows the highest required dredging volume, mainly because dredged sediment is disposed physically close to the dredging locations. These findings indicate that it is difficult to optimise the alternative disposal strategy in advance in a way that limits the dredging volume and its associated costs for the targeted long-term effects and thus, continued adaptation as done within the “flexible” approach remains desirable.

Increasing the minimum channel depth for navigation resulted in an increase in required dredging volume (Fig. 9*b*), but mainly for the first five years. Afterwards, the

Fig. 8. Channel locations for sea-level rise scenarios for a 40 years period determined by the network extraction method for the model runs. (*a*) Control run with no sea-level rise. (*b*) Sea-level rise of 1 mm/year. (*c*) Sea-level rise of 2 mm/year. (*d*) Sea-level rise of 3 mm/year. The map was created in MATLAB.

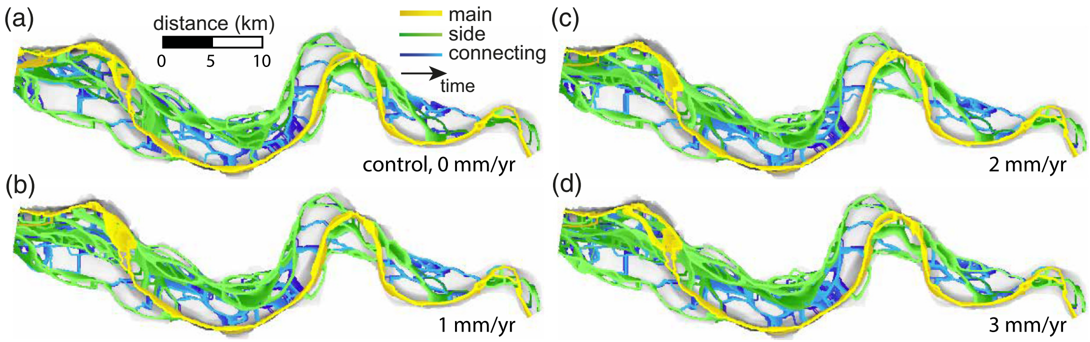

Fig. 9. Dredging volumes per year in the numerical model. (*a*) Modelled dredged volumes for the three disposal strategies, that begin to deviate after 15 years of morphological time. (*b*) Modelled dredged volume increases rapidly with minimum imposed dredging depth at the sills, whereas volumes decrease slightly over time with higher sea-level rise rates.

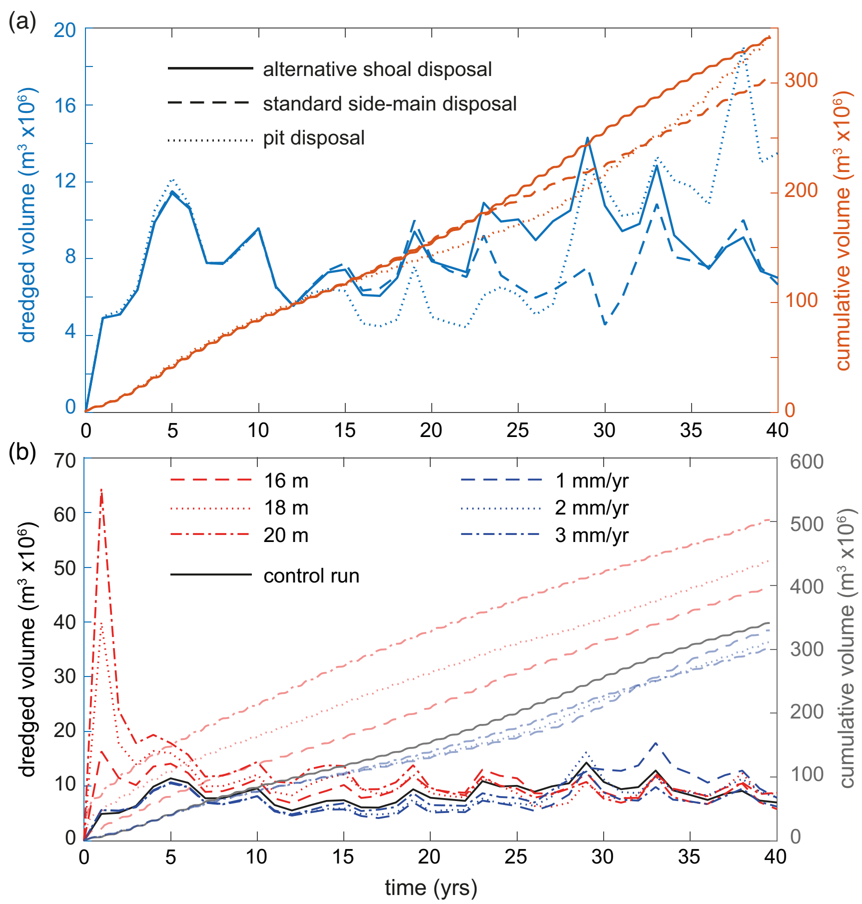

dredging volumes were comparable to the maintenance volumes of the current minimum channel depth. SLR, meanwhile, led to a minor decrease in dredging volume (Fig. 9*b*).

4. Discussion

This discussion includes a description of the effects of dredging on the channels and tidal flats in the estuary, a prospect of what future scenarios hold regarding the adverse effects of dredging and the wider implications of dredging. The effects are described based on the findings in the field and the flume experiments, whereas the future pressures of the estuary are explained by the findings of the model simulations.

4.1. Increasing dominance of the main channel and intertidal flats

The ecological value of estuaries is partly determined by the cumulative area of intertidal flats (Graveland et al. 2005; Desjardins et al. 2012). Particularly, the local physical conditions, i.e., low-dynamic areas, are highly important for ecology in estuaries with a complex spatial configuration of tidal flats, shoals, and channels (Ysebaert et al. 2003; Van der Wal et al. 2017).

Our analogue flume experiments of multi-channel estuaries show that the tidal flats increase in volume (Fig. 10*a*), due to the increase in area as well as in elevation, whilst dredging and disposal is ongoing. This increases the intertidal area and especially the total supratidal area (Fig. 2). Tidal flats that were frequently used as disposal locations increased in volume and elevation, causing an increase in elevation difference with the deeper dredged main channel. While the tidal flat volume recovered somewhat in the undisturbed period after the first dredging activities, the second set of dredging activities pushed the tidal flat volume well away from that of the control experiments.

The bathymetric field data of the heavily dredged Western Scheldt confirms that, as dredging volume increases, the median tidal flat volume calculated from area and elevation tends to increase due to merging of shoals since the 1990s (Figs. 5 and 10*b*), resulting in an increase in intertidal area. The tidal flat elevation above mean sea level (0 m NAP, Amsterdam Ordnance Datum) has increased by half a metre since 1955 and slowed down in the last decade in agreement with other analyses (Wang et al. 2015; De Vet et al. 2017).

Important criteria for the existence of, and the feasibility to maintain, a multi-channel system are the estuarine width-to-depth ratio and flow velocity of the ebb- and flood-dominated channels (Winterwerp et al. 2001; Leuven et al. 2018*b*). In rivers, shallowing of one channel in a multi-channel system usually leads to destabilisation because fluvial bifurcations are unstable in most conditions (Bolla Pittaluga et al. 2015). Shallowing of one of the main (ebb or flood) channels could therefore destabilise the multi-channel system, which would also reduce the number of connecting channels over the intertidal flats (Jeuken and Wang 2010) and the concurrent habitats. This statement should be further tested. The network tool of Hiatt et al. (2020), used in this study, would be able to do a quick assessment in determining the bifurcation angles and its development over sequential digital elevation models.

Flume experiments and field observations consistently show increasing differences in channel depth between the main, side, and connecting channels due to dredging. Dredging deepens one of the channels and causes the side channels to become shallower (Fig. 10*c*). Comparison between dredged and control experiments demonstrate that bed elevation for the main channel becomes significantly deeper than the side and connecting channels in case of dredging, whereas without interference, ebb- and flood-dominated channels form that are equal in size (Fig. 10*c*). This suggests that, in a natural multi-channel system in tide-dominated estuaries with low river discharges, the different channel scales are connected and are equally important, and the imbalance in bed elevation in dredged

Fig. 10. Increasing contrast between the deepening of the main channel and the consolidation of the tidal flats shown by increasing tidal flat volumes, deepening main channels, and shallowing side channels and connecting channels. (*a*) Tidal flat volume for the two experiments. (*b*) Tidal flat volume in the Western Scheldt since 1955. (*c*) Median bed elevation for all three scales of channels for the two experiments. (*d*) Median bed elevation for the main, side, and connecting channels in the Western Scheldt. In (*a*) and (*b*), the percentiles are taken from the distribution of all tidal flat areas encompassed by the channel network, where the 80th percentile represents the more extensive tidal flats.

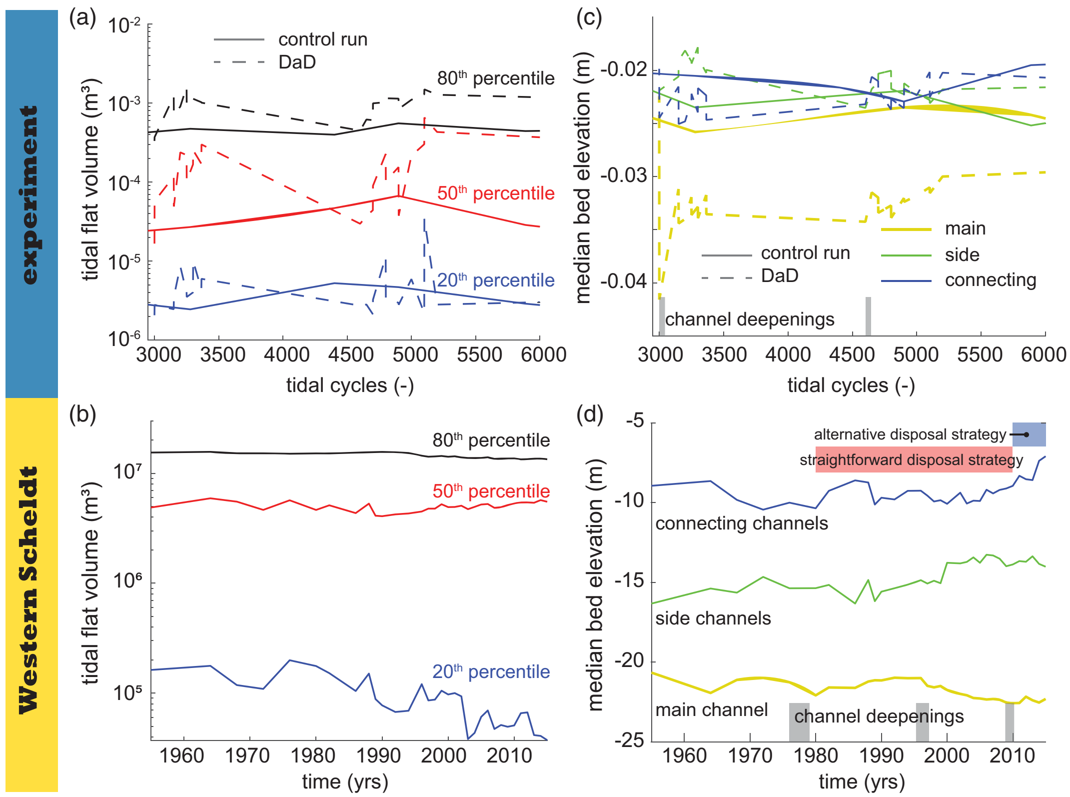

systems is a direct effect of the dredging. Moreover, the difference in channel depth between main and side channels persisted long after dredging was terminated in the experiment. These findings show that dredging leads to an unnatural imbalance among the main, side, and connecting channels in a multi-channel system, and we expect that the consequences are irreversible over the human lifespan.

Field observations confirm that, since dredging started, the main channel became deeper, as expected, especially following major main channel deepening events (the 1970s, 1997–1998, and 2010–2011, to the minimum water depths of 9.5, 11.6, and 14.5 m below LAT (Swinkels et al. 2009), respectively). The volume of dredged sediment disposal into the side channels was reduced when it appeared that this tended to close them off (Swinkels et al. 2009; Jeuken and Wang 2010). The conversion to an alternative tidal flat disposal strategy, where 20% of the dredged sediment was disposed on the seaward end of the intertidal flats, resulted in stabilisation of the channel depth of the side channels, with the intention to improve the ecological valuable habitat. It was hoped that the new strategy would improve the self-erosive capacity of the smaller-scale connecting channels (Roose et al. 2008). However, our network analysis shows that in the last five years, the connecting

Fig. 11. Channel activity and number of channels. (*a*) The migration rate of the main channel for the two experiments (DaD, dredging and disposal). (*b*) Fraction of reworked area in the entire study area over the past 60 years by the main, side, and connecting channels in the Western Scheldt. Note there is a jump in reworked area around 1990 related to changes in the bathymetry data. (*c*) The number of channels for the two experiments. (*d*) The number of channels in the Western Scheldt since 1955.

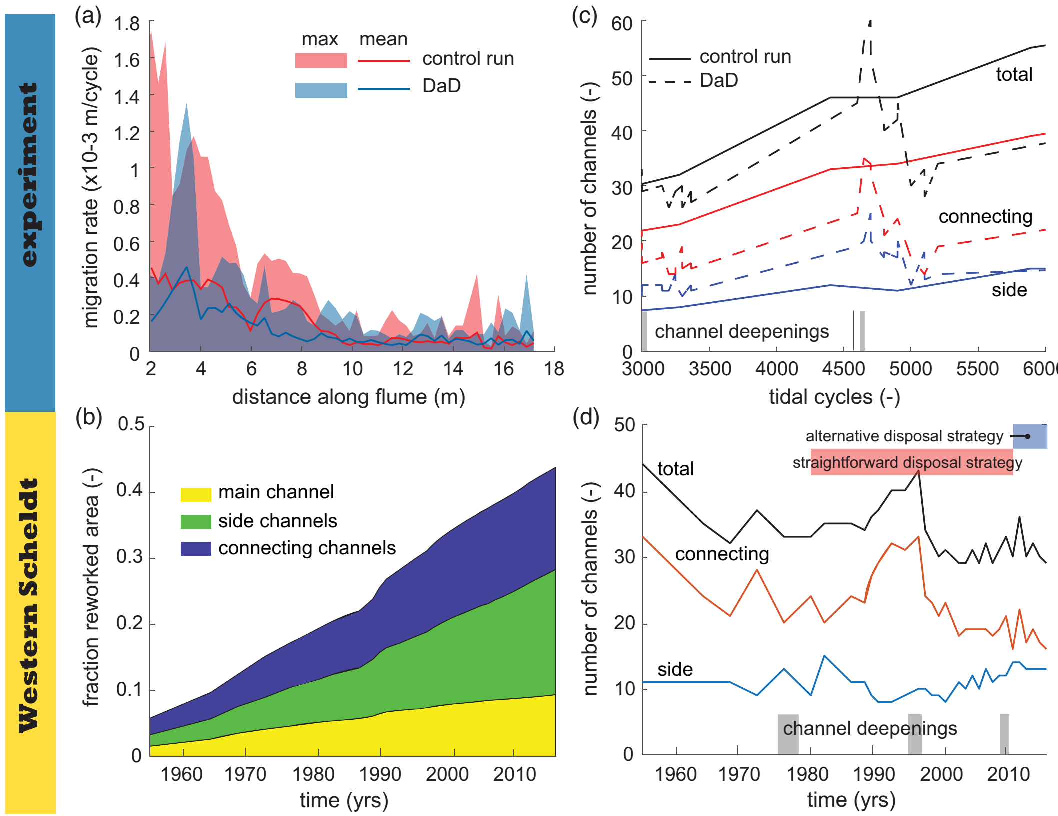

channels continued to silt up (Fig. 10*d*), which could be due to the disposal strategy at the seaward edge of the shoals (see loss of connections in Fig. 4*c*). This development jeopardises the multi-channel nature of the system and the latest strategy fails to preserve the ecologically significant connecting channels.

4.2. Decreasing channel dynamics and loss of connecting channels

Channels and intertidal flats form dynamic elements in natural estuaries (Hibma et al. 2004; Leuven et al. 2018*a*). The dynamics are determined by the displacement and migration of the channels that results in erosion and accretion of the intertidal flats. The flume experiments show that the main channel mainly migrates laterally, because of the decrease in channel displacement and fixation of the main channel by the dredging activity. As result, the meander bend increases in amplitude and sinuosity (Fig. 3*b*). Stabilisation of the meander bend by dredging reduced the migration rate of the main channel in the experiments by 10%–25% (Fig. 11*a*). Channels in the Western Scheldt migrate at different rates depending on channel scale, occupying large portions of the estuary limited by the dikes (Fig. 11*b*). The variation of the main channel location is limited laterally by geological constraints and man-made structures and is furthermore fixed in place by dredging. In contrast, the connecting channels are largely free to migrate as they are not altered or fixed for navigation, whereas side channels which are used for recreational ships can migrate but are limited by human interference and by the estuary geometry that is fixed by the embankments.

Actively disposing dredged sediment at the seaward side of intertidal flats was expected to increase adjacent low-dynamic tidal habitat are and also increase dynamics of the connecting channels (Roose et al. 2008), but surprisingly, the opposite was observed in the field data and experiments. Smaller-scale connecting channels link the large ebb and flood channels. The smaller channels often display a quasi-cyclic morphologic behaviour, characterised by processes of channel origination, migration, and degeneration at a timescale of years to decades (Van Veen 1950; Jeuken 2000). Water level differences between the ebb and flood channels drive the flow of water through these connecting channels. Moreover, connecting channels form where the difference in water levels is the largest, typically in shoal areas at the landward end of the flood channel (Swinkels et al. 2009). The large reduction in dynamics of the connecting channels is demonstrated by the decreasing number of connecting channels since 1955, whilst the number of side channels remained the same or slightly increased (Fig. 11*d*).

This observation is confirmed by the flume experiments, which show a general decrease in the number of channels for the dredged scenarios compared to the control runs (Fig. 11*c*). This is again especially true for the number of connecting channels, which reduces by almost 50% during dredging and remains 10%–20% lower for the period after termination of dredging. Reduction of the dynamics is a problem, because in the field this means that less areas are substantially reworked of their muddy sediment by the migration of the connecting channels. Mud-rich areas are desirable for establishment of valuable habitats (Van der Wal et al. 2017). However, some parts of the estuary may experience the establishment of salt-marsh areas due to the increase of the tidal range and accumulation of mud, which is beneficial for the system. The disposal strategy could also assist in developing more low-dynamic areas that form valuable habitats. The shoal edge disposal strategy did increase the low-dynamic area (Plancke et al. 2017*a*, 2017*b*), which was one of the original reasons to oppose this strategy.

4.3. Effects of future pressures on the estuary

The numerical modelling afforded the possibility to explore effects of future pressures on the estuary development. Since dredging began at early 20th century, the disposal strategy has evolved with the aim of counteracting the adverse effects of dredging. Model runs for an alternative tidal flat disposal strategy show very little difference with the previous, straightforward strategy (Figs. 12*a* and 12*b*). For the near future, a new strategy was proposed to dispose dredged sediments in the deep scours of the main channel (Huisman et al. 2018). Our model simulations for this strategy of dredged sediment disposal solely in scours of the main channel, indicate that this reduces the adverse effect of decreasing channel dynamics (Fig. 12*a*) and halts the increase in tidal flat volume (Fig. 12*b*). In case of the Western Scheldt, the total scour volume available for disposal is 1.7×10^9 m^3. This was calculated by the difference between the current navigation depth of 14.5 m LAT and the actual depth at all scours in the Western Scheldt, including the deep scours at Vlissingen and Borssele, and assuming no limitation by the allowed permits. This means that with a disposal rate of 10×10^6 m^3, it will take at least 100 years to fill the deep scours, assuming that the sediment simply fills the scours and is not transported out. The presence of the scours suggests that sediment was transported out from these areas of the river bed and this promising disposal strategy has been tested (Huisman et al. 2020; Huismans et al. 2020; Stark et al. 2020), which is discussed later in section 4.4.

Fig. 12. Effect of future scenarios on channel dynamics, expressed as reworked area, and ecologically valuable waterline length, represented by intertidal flat volume. The effect is compared against a control run, and therefore shows a relative effect. (*a*) Effect of disposal strategy on changes in the reworked area. (*b*) Effect of disposal strategy on changes in tidal flat volume. (*c*) Effect of dredging depth on changes in the reworked area. (*d*) Effect of dredging depth on changes in tidal flat volume. (*e*) Effect of sea-level rise on changes in the reworked area. (*f*) Effect of sea-level rise on changes in tidal flat volume.

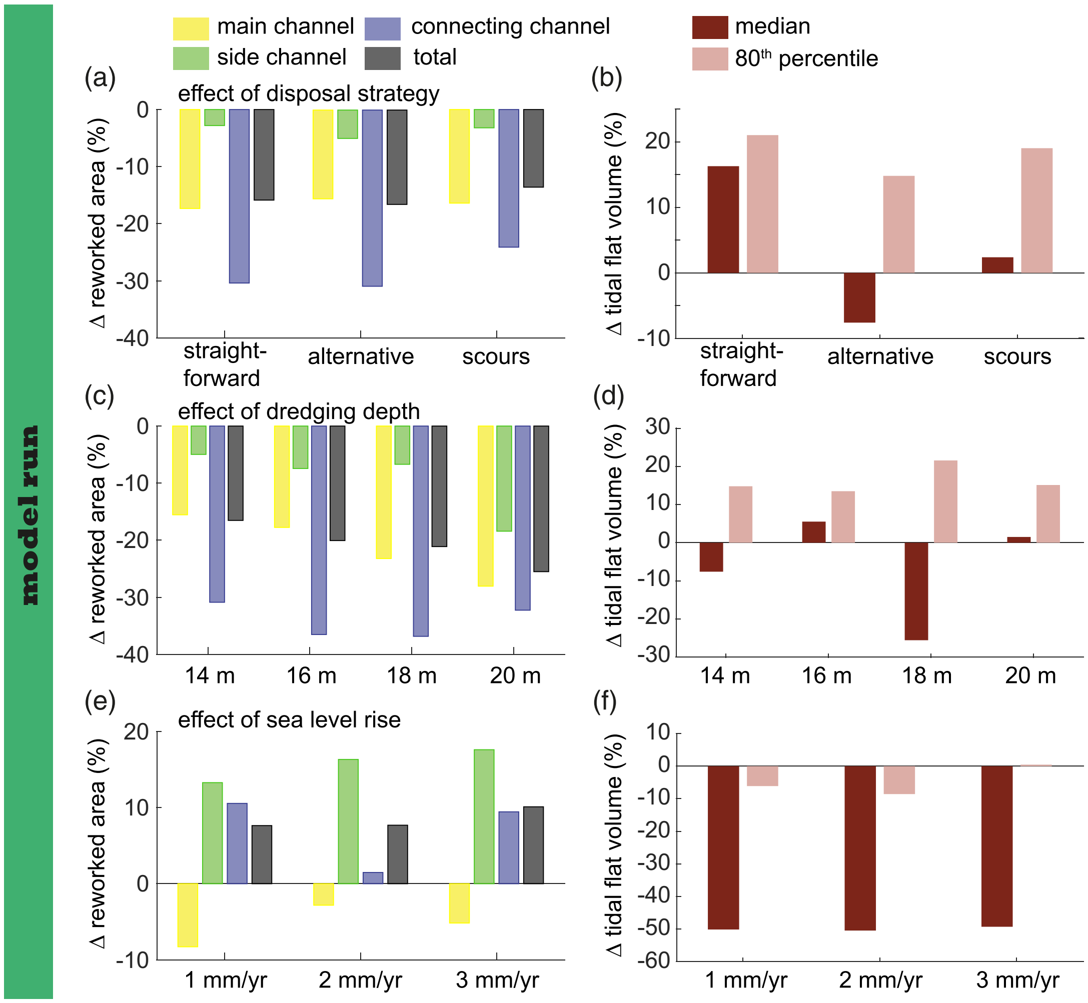

Increasing vessel draft (Rodrigue et al. 2017) brings further management challenges. Increasing the minimum main channel depth in the model simulation shows decreasing dynamics of the main channel, whereas there appears to be a minimum in connecting channel dynamics (Fig. 12*c*). While channel dynamics decrease with dredging depth, there is no systematic increase in tidal flat volume with dredging depth. The tidal flat volume is annually 10%–25% higher for 16–20 m water depth, respectively (Fig. 12*d*). We argue that further deepening of the shipping fairway for short-term economic purposes should be carefully evaluated against long-term ecological value, as a further decrease in channel dynamics will directly affect intertidal flat dimensions and therefore valuable habitat area as shown by past developments in the Western Scheldt and by scenarios in the numerical modelling and experiments.

Future threats from SLR are expected in estuarine systems (Blott et al. 2006; Leuven et al. 2019) and should be a key issue in future assessments for understanding the dynamic response of channel-shoal interactions in estuaries. Here, we systematically evaluate the response of the estuary to various SLR scenarios based on the Intergovernmental Panel on Climate Change Fifth Assessment Report (Church et al. 2013). We expect that SLR has less effect on the channel-shoal interactions compared to the deepening of the shipping fairway because the rates are small compared to the draft depth rate of 140 mm/year for the container-vessels. The growth of an estuary with SLR depends on the sediment supply that needs to be sufficient from the seaward or landward side (Leuven et al. 2019). For the Western Scheldt that is flood-asymmetric, sediment is mainly imported from sea. We expect that modest SLR will transport additional sediment into the estuary. The model simulations showed a doubling of coastal sediment input for the lower bound of SLR, up to 150% increase for the upper bound of SLR, based on bed elevation differences after 40 years morphological development. The actual import will partly depend on ebb delta dynamics, alongshore drift, sediment availability, and changes in tidal amplitude due to shifting offshore amphidromic points (Leuven et al. 2019), none of which are considered in the present model runs. The model scenarios show that limited future SLR will cause a valuable increase in dynamics of the side and connecting channels, though the main channel becomes even further fixated (Fig. 12*e*). Intertidal flat elevation increases with the SLR in the model run whilst tidal flat volume decreases (Fig. 12*f*).

4.4. Management recommendations and wider application

Human intervention is very common in estuaries around the world. The morphology of estuaries including location and presence of bars and shoals, amount of intertidal flats, number of channels, and side channels are directly impacted by these human interventions. Model simulations reveal that current dredging strategies are not sustainable, and current disposal strategies to counter adverse effects are, however, limited in their effectiveness. Moreover, the experiments suggest that channel–shoal interactions in anthropogenically altered estuaries are affected for a much longer time-span than the period of dredging.

We argue that not only dredging but also, the disposal strategies are equally important for maintaining suitable conditions for the ecologically valuable multi-channel system to persist (Boyd et al. 2000; Jensen and Mogensen 2000; Wang et al. 2015). For the Western Scheldt estuary, the disposal strategy has changed over the years. A promising strategy could be the scour disposal strategy whereby dredged sediment is disposed in the scours of the main channel (Huisman et al. 2018). The effectiveness of the strategy depends, however, on future developments such as increasing vessel draft, SLR, and economic impact. For instance, if disposed material is instantly washed away, dredging intensity increases. This, however, is not the case for the pilot projects (Huismans et al. 2020; Huisman et al. 2020; Stark et al. 2020), nor do the dredging volumes in this study show an increase in the intensity. Overall, the pilot test of the scour disposal project showed that sediment is transported mainly to the inner bend (Huisman et al. 2020; Huismans et al. 2020), which increases the chance of shoal margin collapses which have been proven to be common in the study area (Van Dijk et al. 2018). Shoal margin collapses lead to sediment deposition back in the scour. Regarding the multi-channel system, the scour disposal strategy limits the shallowing of side channels (Huisman et al. 2020), which is an improvement compared to the shoal edge disposal strategy. Still, there are some questions remaining concerning the scour disposal strategy and how it can and will work as numerical models struggle to reproduce the hydrodynamics and sediment stability in these scours (Huisman et al. 2020;

Stark et al. 2020), therefore, continuous monitoring is necessary to further understand the advantages and disadvantages (Huismans et al. 2020).

We would argue that further deepening of the main channel should be carefully considered against adverse effects. In view of future SLR, it is highly advisable that the sediment be kept in the system rather than mined or disposed of outside the system. A further decrease in channel dynamics and displacement destabilises the valuable multi-channel system, including intertidal flats, which determines the existence and persistence of the ecologically important habitat, and the depth of side channels for navigability of smaller inland vessels (Nichols 2018). Furthermore, dredging increases the tidal range resulting in higher flood risk, alters ebb-flood dominance, and peak velocity increases that complicates navigability (Liria et al. 2009; Colby et al. 2010; Leuven et al. 2019). On the other hand, the increase in channel dynamics associated with SLR provides an opportunity to restore ecologically valuable areas, by increasing intertidal flats and the number of connecting channels that flow through and feed these systems, which may also help to adapt the system to the SLR (Kirwan et al. 2016; Leuven et al. 2019).

5. Conclusions

We presented three methods to study the effect of dredging and disposal on the multi-channel character of an estuary and on the area of ecological valuable intertidal flats within the estuary. For this study, we used a network extraction method that determines automatically the channel network from the bed elevation. The applied network extraction method facilitates the quantification of channel dynamics and the multi-channel character of the system. We show that in systems with dredging, the number of channels and the dynamics of channels decreases for the experiment, field observations, and model study. Due to amalgamation, i.e., merging, of the intertidal flats, the total area of intertidal flats increases, but the circumference of the intertidal flat reduces, which has a consequence on the ecological value of the intertidal flat. The current flexible disposal strategy in the Western Scheldt is successful in sustaining the multi-channel character of the system. However, increasing dredging depth for shipping may cause a further imbalance between the main and side channels within the multi-channel system. This will probably further reduce the dynamics of the system. Meanwhile, additional sediment import (assuming sufficient sediment availability) due to SLR could restore the balance somewhat by increasing the dynamics of the system.

From our laboratory experiments, field data, and numerical model study, we conclude that fairway dredging decreases the dynamics of all channels and the area of ecologically valuable tidal flats. The current disposal strategy that aims to reduce these effects is not sufficient to restore the natural equilibrium. Further deepening of the navigation channel will accelerate the adverse effects of dredging, whereas SLR scenarios show potential improvement of channel dynamics and intertidal flat volumes. These findings show that dredging leads to an unnatural imbalance among the main, side, and connecting channels in a multi-channel system, and based on the laboratory experiments, we expect that the consequences are irreversible within the human lifespan.

Acknowledgements

W.M. van Dijk, J.R.F.W. Leuven, and M.G. Kleinhans were supported by the Dutch Technology Foundation TTW under project No. STW-Vici-016.140.316/13710 (granted to M.G. Kleinhans), which is part of the Netherlands Organisation for Scientific Research (NWO). M.R. Hiatt was supported by an ERC Consolidator Grant (agreement 647570) awarded to M.G. Kleinhans. W. Sonke and B. Speckmann were supported by the Netherlands Organisation for Scientific Research (NWO) under project No. 639.023.208

(Vici granted to B. Speckmann), K. Verbeek under project No. 639.021.541. W.M.D. managed the numerical model simulations. J.R.C. and J.R.F.W.L. conducted the physical scale experiments. J.C. and M.T. contributed to background information and data of the Western Scheldt. M.R.H, W.S., K.V., and B.S. developed and tested the network extraction tool. W.M.D., J.R.C., J.R.F.W.L., and M.G.K. provided critical result interpretation. W.M.D. wrote the initial draft of the paper, with substantial contributions from all authors. B.S. led network extraction research and M.G.K. led modelling and experimental research. We gratefully acknowledge Marco Schrijver and Gert-Jan Liek (Rijkswaterstaat Zee en Delta) for insightful discussions. Constructive and positive reviews by two anonymous reviewers, Associate Editor Shari Gallop, and guidance by Editor Ian Townend helped to clarify and strengthen the manuscript. The Delft3D model software is open source, and the code is available from the Deltares website (https://oss.deltares.nl/web/delft3d). All field data from Rijkswaterstaat are publicly available from a variety of web portals or via the service desk (https://www.rijkswaterstaat.nl/zakelijk/open-data). The network tool is called TTGA: Topological Tools for Geomorphological Analysis and available at https://doi.org/10.5281/zenodo.3634684.

References

Baar, A.W., Boechat Albernaz, M., van Dijk, W.M., and Kleinhans, M.G. 2019. Critical dependence of morphodynamic models of fluvial and tidal systems on empirical downslope sediment transport. Nat. Commun. **10**: 4903. doi:10.1038/s41467-019-12753-x. PMID:31653869.

Best, J. 2019. Anthropogenic stresses on the world's big rivers. Nat. Geosci. **12**: 7–21. doi:10.1038/s41561-018-0262-x.

Blott, S.J., Pye, K., Van der Wal, D., and Neal, A. 2006. Long-term morphological change and its causes in the Mersey Estuary, NW England. Geomorphology, **81**(1–2): 185–206. doi:10.1016/j.geomorph.2006.04.008.

Bolla Pittaluga, M., Coco, G., and Kleinhans, M.G. 2015. A unified framework for stability of channel bifurcations in gravel and sand fluvial systems. Geophys. Res. Lett. **42**(18): 7521–7536. doi:10.1002/2015GL065175.

Boyd, S.E., Rees, H.L., and Richardson, C.A. 2000. Nematodes as sensitive indicators of change at dredged material disposal sites. Estuar. Coast. Shelf Sci. **51**: 805–819. doi:10.1006/ecss.2000.0722.

Braat, L., Leuven, J.R.F.W., Lokhorst, I.R., and Kleinhans, M.G. 2018. Effects of estuarine mudflat formation on tidal prism and large-scale morphology in experiments. Earth Surf. Process. Landf. **44**(2): 417–432. doi:10.1002/esp.4504.

Cancino, L., and Neves, R. 1999. Hydrodynamic and sediment suspension modelling in estuarine systems. J. Mar. Syst. **22**: 117–131. doi:10.1016/S0924-7963(99)00036-6.

Chen, Y., Dong, J., Xiao, X., Zhang, M., Tian, B., Zhou, Y., et al. 2016. Land claim and loss of tidal flats in the Yangtze Estuary. Sci. Rep. **6**(1): 24018. doi:10.1038/srep24018.

Church, J.A., Clark, P.U., Cazenave, A., Gregory, J.M., Jevrejeva, S., Levermann, A., et al. 2013. Sea-level rise by 2100. Science, **342**(6165): 1445. doi:10.1126/science.342.6165.1445-a. PMID:24357297.

Cleveringa, J. 2013. LTV — Veiligheid en Toegankelijkheid: Ontwikkeling mesoschaal Westerschelde (factsheets). Technical report. International Mairne & Dredging Consultants, Deltares, Svašek Hydraulics BV and ARCADIS [In Dutch].

Colby, L.H., Maycock, S.D., Nelligan, F.A., Pocock, H.J., and Walker, D.J. 2010. An investigation into the effect of dredging on tidal asymmetry at the River Murray mouth. J. Coast. Res. **265**(5): 843–850. doi:10.2112/08-1143.1.

Dam, G. 2017. Lange-termijn sedimentbalans Westerschelde. Technical report. SVASEK Hydraulics [In Dutch].

Depreiter, D., Sas, M., Beirinckx, K., and Liek, G.-J. 2011. Flexible disposal strategy: Monitoring as a key to understanding and steering environmental responses to dredging and disposal in the Scheldt Estuary. *In* Taking Care of the Sea: Conference Proceedings of Hydro12, Rotterdam, the Netherlands. pp. 1–8.

Depreiter, D., Lanckriet, T., Van Holland, G., Vanlede, J., Beirinckx, K., and Maris, T. 2015. Mud disposal and suspended sediment concentration in the Lower Sea Scheldt — Towards a hyperturbid system? *In* E-proceedings of the 36th IAHR World Congress, The Hague, the Netherlands. pp. 38–52.

Desjardins, P.R., Buatois, L.A., and Màngano, M.G. 2012. Chapter 18 — Tidal flats and subtidal sand bodies. *In* Trace fossils as indicators of sedimentary environments. Vol. 64. Developments in Sedimentology. *Edited by* D. Knaust and R.G. Bromley. Elsevier. pp. 529–561.

De Vet, P.L.M., Van Prooijen, B.C., and Wang, Z.B. 2017. The difference in morphological development between the intertidal flats of the Eastern and Western Scheldt. Geomorphology, **281**: 31–42. doi:10.1016/j.geomorph.2016.12.031.

De Vriend, H.J., Wang, Z.B., Ysebaert, T., Herman, P.M.J., and Ding, P. 2011. Ecomorphological problems in the Yangtze Estuary and the Western Scheldt. Wetlands, 31: 1033–1042. doi:10.1007/s13157-011-0239-7.

Edelsbrunner, H., Harer, J., and Zomorodian, A. 2001. Hierachical morse complexes for piecewise linear 2-manifolds. *In* Proceedings of the 17th Annual Symposium on Computational Geometry. SCG '01, New York, NY, USA. ACM. pp. 70–79.

Elias, E.P.L., Van der Spek, A.J.F., and Lazar, M. 2017. The 'Voordelta', the contiguous ebb-tidal deltas in the SW Netherlands: Large-scale morphological changes and sediment budget 1965–2013; impacts of large-scale engineering. Neth. J. Geosci. **96**(3): 233–259. doi:10.1017/njg.2016.37.

Essink, K. 1999. Ecological effects of dumping of dredged sediments; options for management. J. Coast. Conserv. **5**(1): 69–80. doi:10.1007/BF02802741.

Graveland, J., Van Eck, G.T.M., Kater, B.J., Liek, G.J., and van Maldegem, D.C. 2005. Fysische en ecologische kennis en modellen voor de Westerschelde: wat is beleidsmatig nodig en wat is beschikbaar voor de m.e.r. Verruiming Vaargeul? Technical report. Rapport RIKZ/2005.018. Rijkswaterstaat, Rijksinstituut voor Kust en Zee, Middelburg, the Netherlands [In Dutch].

Gruijters, S.H.L.L., Schokker, J., and Veldkamp, J.G. 2004. Kartering moeilijk erodeerbare lagen in het Schelde estuarium. Rapport NITG 03213B1208. TNO [In Dutch].

Hartsuiker, G. 2004. 2Dh NEVLA-Scheldemodel: bouw en afregeling stromingsmodel. Technical report. Alkyon, Emeloord, the Netherlands.

Hiatt, M., Sonke, W., Addink, E.A., van Dijk, W.M., van Kreveld, M., Ophelders, T., et al. 2020. Geometry and topology of estuary and braided river channel networks automatically extracted from topographic data. J. Geophys. Res.: Earth Surf. **125**(1): e2019JF005206. doi:10.1029/2019JF005206. PMID:32714724.

Hibma, A., Schuttelaars, H.M., and De Vriend, H.J. 2004. Initial formation and long-term evolution of channel-shoal patterns. Cont. Shelf Res. **24**(15): 1637–1650. doi:10.1016/j.csr.2004.05.003.

Hibma, A., Wang, Z.B., Stive, M.J.F., and De Vriend, H.J. 2008. Modelling impact of dredging and dumping in ebb-flood channel systems. Trans. Tianjin Univ. **14**(4): 271–281. doi:10.1007/s12209-008-0047-1.

Huisman, B., Schrijvershof, R., Lanckriet, T., and van der Werf, J. 2018. Baggerdepositie in diepe geulen: strategie voor het plaasten van gebaggerd materiaal in de diepere getijdegeulen van de Westerschelde. Technical report. Deltares [In Dutch].

Huisman, B.I.A., Huismans, Y., and Vroom, J. 2020. Effecten van storten in diepe putten van de Westerschelde: Synthese van proefstortingen en modelanalyses. Technical report. Deltares, Delft, the Netherlands.

Huismans, Y., Van der Vegt, H., Huisman, B.I.A., and Alonso, A.C. 2020. Westerschelde: storten in diepe putten Technische rapportage: mesoschaal morfologische ontwikkelingen rond de Put van Hansweert. Technical report. Deltares, Delft, the Netherlands.

Jensen, A., and Mogensen, B. 2000. Effects, ecology and economy. *In* Environmental aspects of dredging — Guide No. 6. International Association of Dredging Companies (IADC) and Central Dredging Association (CEDA). p. 119.

Jeuken, M.C.J.L. 2000. On the morphologic behaviour of the tidal channels in the Westerschelde estuary. Ph.D. thesis, Universiteit Utrecht.

Jeuken, M.C.J.L., and Wang, Z.B. 2010. Impact of dredging and dumping on the stability of ebb–flood channel systems. Coast. Eng. **57**: 553–566. doi:10.1016/j.coastaleng.2009.12.004.

Kerner, M. 2007. Effects of deepening the Elbe Estuary on sediment regimen and water quality. Estuar. Coast. Shelf Sci. **75**(4): 492–500. doi:10.1016/j.ecss.2007.05.033.

Kirwan, M.L., Temmerman, S., Skeehan, E.E., Guntenspergen, G.R., and Fagherazzi, S. 2016. Overestimation of marsh vulnerability to sea level rise. Nat. Clim. Change, **6**: 253–260. doi:10.1038/nclimate2909.

Kleinhans, M.G. 2005. Flow discharge and sediment transport models for estimating a minimum timescale of hydrological activity and channel and delta formation on Mars. J. Geophys. Res. **110**: E12003. doi:10.1029/2005JE002521.

Kleinhans, M.G., Kreveld, M., Ophelders, T., Sinke, W., Speckmann, B., and Verbeek, K. 2017*a*. Computing representative networks for braided rivers. *In* 33rd International Symposium on Computational Geometry (SoCG 2017). Vol. 77. Leibniz International Proceedings in Informatics (LIPIcs). *Edited by* B. Aronov and M.J. Katz. Schloss Dagstuhl–Leibniz-Zentrum fuer Informatik. pp. 48:1–48:16.

Kleinhans, M.G., van der Vegt, M., Leuven, J., Braat, L., Markies, H., Simmelink, A., et al. 2017*b*. Turning the tide: Comparison of tidal flow by periodic sea level fluctuation and by periodic bed tilting in scaled landscape experiments of estuaries. Earth Surf. Dyn. **5**: 731–756. doi:10.5194/esurf-5-731-2017.

Kleinhans, M.G., van Kreveld, M., Ophelders, T., Sonke, W., Speckman, B., and Verbeek, K. 2019. Computing representative networks for braided rivers. J. Comput. Geom. **10**(1): 423–443. doi:10.20382/jocg.v10i1a14.

Lesser, G.R., Roelvink, J.A., Van Kester, J.A.T.M., and Stelling, G.S. 2004. Development and validation of a three-dimensional morphological model. Coast. Eng. **51**(8–9): 883–915. doi:10.1016/j.coastaleng.2004.07.014.

Leuven, J.R.F.W., Braat, L., van Dijk, W.M., De Haas, T., Van Onselen, E.P., Ruessink, B.G., and Kleinhans, M.G. 2018*a*. Growing forced bars determine nonideal estuary planform. J. Geophys. Res.: Earth Surf. **123**(11): 2971–2992. doi:10.1029/2018JF004718.

Leuven, J.R.F.W., De Haas, T., Braat, L., and Kleinhans, M.G. 2018*b*. Topographic forcing of tidal sand bar patterns for irregular estuary planforms. Earth Surf. Process. Landf. **43**(1): 172–186. doi:10.1002/esp.4166.

Leuven, J., Pierik, H.-J., Van der Vegt, M., Bouma, T., and Kleinhans, M.G. 2019. Sea-level-rise-induced threats on the size of tide-influenced estuaries worldwide. Nat. Clim. Change, **9**: 986–992. doi:10.1038/s41558-019-0608-4.

Liria, P., Garel, E., and Uriarte, A. 2009. The effects of dredging operations on the hydrodynamics of an ebb tidal delta: Oka Estuary, northern Spain. Cont. Shelf Res. **29**(16): 1983–1994. doi:10.1016/j.csr.2009.01.014.

Maximova, T., Ides, S., De Mulder, T., and Mostaert, F. 2009*a*. LTV O & M thema Veiligheid — Deelproject 1: Verbetering hydrodynamisch NeVla model ten behoeve van scenario-analyse. WL rapporten 756_05. Flanders Hydraulics Research & Deltares, Antwerp, Belgium [In Dutch].

Maximova, T., Ides, S., De Mulder, T., and Mostaert, F. 2009*b*. Verbetering randvoorwaardenmodel. Deelrapport 4: Extra aanpassingen Zeeschelde. WL rapporten 753_09. Flanders Hydraulics Research, Antwerp, Belgium [In Dutch].

Maximova, T., Ides, S., Vanlede, J., De Mulder, T., and Mostaert, F. 2009*c*. Verbetering 2D randvoorwaardenmodel. Deelrapport 3: kalibratie bovenlopen. WL rapporten 753_09. Flanders Hydraulics Research, Antwerp, Belgium [In Dutch].

Monge-Ganuzas, M., Cearreta, A., and Evans, G. 2013. Morphodynamic consequences of dredging and dumping activities along the Lower Oka estuary (Urdaibai Biosphere Reserve, southeastern Bay of Biscay, Spain). Ocean Coast. Manage. **77**: 40–49. doi:10.1016/j.ocecoaman.2012.02.006.

MOW. 2013. Work package 5 'measures': Dredging and diposal strategies. Technical report. TIDE project.

Nichols, M.M. 2018. Consequences of dredging. *In* Hydrodynamics of estuaries: Volume II Estuarine case studies. *Edited by* B. Kjerfve. CRC Press.

Plancke, Y., Beirinckx, K., Liek, G.J., Vos, G.R., and Schrijver, M. 2014. A new disposal strаregy for the Western Scheldt, conciliating port accessibility and nature preservation. *In* 2nd PIANC Congress, 125th Anniversary PIANC — Setting the Course, Liverpool, UK. PIANC.

Plancke, Y., De Schrijver, M., Meire, D., and Mostaert, F. 2017*a*. Overleg Flexibel Storten: deelrapport 20. Analyse van de waterbeweging, het sedimenttransport en de morfologie nabij de Hooge Platen. Technical report. Waterkundig Laboratorium and Rijkswaterstaat Zee en Delta, Antwerp, Belgium.

Plancke, Y., De Schrijver, M., Meire, D., and Mostaert, F. 2017*b*. Overleg Flexibel Storten: deelrapport 22. Analyse van de waterbeweging, het sedimenttransport en de morfologie nabij de Plaat van Walsoorden. Technical report. Waterkundig Laboratorium and Rijkswaterstaat Zee en Delta, Antwerp, Belgium.

Rodrigue, J.-P., Comtois, C., and Slack, B. 2017. The geography of transport systems. Routledge, London, UK and New York, N.Y., USA.

Roose, F., Plancke, Y., and Ides, S. 2008. A synthesis on the assessment of an alternative disposal strategy to serve sustainability in the Scheldt estuary. *In* CEDA Dredging Days 2008: Dredging Facing Sustainability, Antwerp, Belgium. pp. 1–13.

Schrijvershof, R., and Vroom, J. 2016. Effecten van realistische (extreme) stortstrategieën in de Westerschelde. Technical report. Deltares [In Dutch].

Schuurman, F., Kleinhans, M.G., and Marra, W.A. 2013. Physics-based modeling of large braided sand-bed rivers: Bar pattern formation, dynamics, and sensitivity. J. Geophys. Res.: Earth Surf. **118**: 2509–2527. doi:10.1002/2013JF002896.

Smolders, S., Maximova, T., Vanlede, J., Plancke, Y., Verwaest, T., and Mostaert, F. 2016. Integraal Plan Bovenzeeschelde: Subreport 1 — SCALDIS: A 3D hydrodynamic model for the Scheldt Estuary. Technical report. Flanders Hydraulics Research, Antwerp, Belgium.

Stark, J., De Maerschalck, B., Plancke, Y., and Mostaert, F. 2020. Agenda voor de Toekomst — Sedimenttransport op verschillende tijdschalen: Scenario's stortingen diepe delen. Technical report. Waterbouwkundig Laboratorium, Antwerp, Belgium.

Swinkels, C.M., Jeuken, M.C.J.L., Wang, Z.B., and Nicholls, R.J. 2009. Presence of connecting channels in the Western Scheldt Estuary. J. Coast. Res. **253**: 627–640. doi:10.2112/06-0719.1.

Temmerman, S., Govers, G., Wartel, S., and Meire, P. 2004. Modelling estuarine variations in tidal marsh sedimentation: Response to changing sea level and suspended sediment concentrations. Mar. Geol. **212**: 1–19. doi:10.1016/j.margeo.2004.10.021.

Temmerman, S., Meire, P., Bouma, T.J., Herman, P.M.J., Ysebaert, T., and De Vriend, H.J. 2013. Ecosystem-based coastal defence in the face of global change. Nature, **504**: 79–83. doi:10.1038/nature12859. PMID:24305151.

Toffolon, M., and Crosato, A. 2007. Developing macroscale indicators for estuarine morphology: The case of the Scheldt estuary. J. Coast. Res. **231**(1): 195–212. doi:10.2112/03-0133.1.

Van de Lageweg, W.I., and Slangen, A.B.A. 2017. Predicting dynamic coastal delta change in response to sea-level rise. J. Mar. Sci. Eng. **5**(2): 24. doi:10.3390/jmse5020024.

Van de Lageweg, W.I., Braat, L., Parsons, D., and Kleinhans, M. 2018. Controls on mud distribution and architecture along the fluvial-to-marine transition. Geology, **46**: 971–974. doi:10.1130/G45504.1.

Van der Spek, A.J.F. 1997. Tidal asymmetry and long-term evolution of Holocene tidal basins in the Netherlands. Mar. Geol. **141**(1–4): 71–90. doi:10.1016/S0025-3227(97)00064-9.

Van der Wal, D., Lambert, G.I., Ysebaert, T., Plancke, Y.M.G., and Herman, P.M.J. 2017. Hydrodynamic conditioning of diversity and functional traits in subtidal estuarine macrozoobenthic communities. Estuar. Coast. Shelf Sci. **197**: 80–92. doi:10.1016/j.ecss.2017.08.012.

Van Dijk, W.M., Mastbergen, D.R., Van de Ham, G.A., and Kleinhans, M.G. 2018. Location and probability of shoal margin collapses in a sandy estuary. Earth Surf. Process. Landf. **43**(11): 2342–2357. doi:10.1002/esp.4395.

Van Dijk, W.M., Hiatt, M., Van der Werf, J.J., and Kleinhans, M.G. 2019. Effects of shoal margin collapses on the morphodynamics of a sandy estuary. J. Geophys. Res.: Earth Surf. **124**(1): 195–215. doi:10.1029/2018JF004763. PMID:31007991.

Vanlede, J., Clerq, B.D., Decrop, B., Ides, S., van Holland, G., Mulder, T.D., and Mostaert, F. 2009. Permanente verbetering modelinstrumentarium. Verbetering Randvoorwaardenmodel. Deelrapport 2: Afregeling van het 2D Scheldemodel. Technical report. Waterkundig Laboratorium and IMDC, Antwerp, Belgium.

Van Maren, D., Van Kessel, T., Cronin, K., and Sittoni, L. 2015. The impact of channel deepening and dredging on esuarine sediment concentration. Cont. Shelf Res. **95**: 1–14. doi:10.1016/j.csr.2014.12.010.

Van Rijn, L.C. 2007*a*. Unified view of sediment transport by currents and waves. I: Initiation of motion, bed roughness, and bed-load transport. J. Hydraul. Eng. **133**(6): 649–667. doi:10.1061/(ASCE)0733-9429(2007)133:6(649).
Van Rijn, L.C. 2007*b*. Unified view of sediment transport by currents and waves. II: Suspended transport. J. Hydraul. Eng. **133**(6): 668–689. doi:10.1061/(ASCE)0733-9429(2007)133:6(668).
Van Veen, J. 1948. Dredgers' work. *In* Dredge drain reclaim. Springer, Dordrecht, the Netherlands. pp. 60–104.
Van Veen, J. 1950. Ebb and flood channel systems in the Netherlands tidal waters. J. R. Dutch Geogr. Soc. **67**: 303–325 [In Dutch].
Vikolainen, V., Bressers, H., and Lulofs, K. 2014. A shift toward building with nature in the dredging and port development industries: Managerial implications for project in or near Natura 2000 areas. Environ. Manage. **54**(1): 3–13. doi:10.1007/s00267-014-0285-z. PMID:24809286.
Vroom, J., De Vet, P.L.M., and Van der Werf, J.J. 2015. Validatie waterbeweging Delft3D NeVla model Westerscheldemonding. Technical report. Deltares [In Dutch].
Wang, Y., Straub, K.M., and Hajek, E.A. 2011. Scale-dependent compensational stacking: An estimate of autogenic time scales in channelized sedimentary deposits. Geology, **39**: 811–814. doi:10.1130/G32068.1.
Wang, Z.B., Maren, D.S.V., Ding, P.X., Yang, S.L., Prooijen, B.C.V., Vet, P.L.M.D., et al. 2015. Human impacts on morphodynamic thresholds in estuarine systems. Cont. Shelf Res. **111**: 174–183. doi:10.1016/j.csr.2015.08.009.
Winterwerp, J.C., Wang, Z.B., Stive, M.J.F., Arends, A., Jeuken, C., Kuijper, C., and Thoolen, P.M. 2001. A new morphological schematisation of the Western Scheldt Estuary, the Netherlands. *In* Proceedings of the 2nd IAHR Symposium on River, Coastal and Estuarine Morphodynamics. Vol. 6, pp. 1–10.
Ysebaert, T., Herman, P., Meire, P., Craeymeersch, J., Verbeek, H., and Heip, C. 2003. Large-scale spatial patterns in estuaries: Estuarine macrobenthic communities in the Schelde estuary, NW Europe. Estuar. Coast. Shelf Sci. **57**(1): 335–355. doi:10.1016/S0272-7714(02)00359-1.
Yuan, R., and Zhu, J. 2015. The effects of dredging on tidal range and saltwater intrusion in the Pearl River Estuary. J. Coast. Res. **316**(6): 1357–1362. doi:10.2112/JCOASTRES-D-14-00224.1.
Zhu, J., Weisberg, R., and Zheng, L. 2015. Influences of channel deepening and widening on the tidal and nontidal circulations of Tampa Bay. Estuar. Coasts, **38**(1): 132–150. doi:10.1007/s12237-014-9815-4.